

Microscopic simulation of superconductor-topological insulator proximity structures

Mahmoud Lababidi and Erhai Zhao

Department of Physics and Astronomy, George Mason University, Fairfax, Virginia, USA

(Dated: November 13, 2018)

We present microscopic, self-consistent calculations of the superconducting order parameter and pairing correlations near the interface of an s -wave superconductor and a three-dimensional topological insulator with spin-orbit coupling. We discuss the suppression of the order parameter by the topological insulator and show that the equal-time pair correlation functions in the triplet channel, induced by spin-flip scattering at the interface, are of $p_x \pm ip_y$ symmetry. We verify that the spectrum at sub-gap energies is well described by the Fu-Kane model. The sub-gap modes are viewed as interface states with spectral weight penetrating well into the superconductor. We extract the phenomenological parameters of the Fu-Kane model from microscopic calculations, and find they are strongly renormalized from the bulk material parameters. This is consistent with previous results of Stanescu et al for a lattice model using perturbation theory in the tunneling limit.

PACS numbers: 73.20.-r, 75.70.Tj, 85.75.-d

I. INTRODUCTION

Fu and Kane showed that at the interface between a three-dimensional topological band insulator (TI) and an s -wave superconductor (S) forms a remarkable two-dimensional non-Abelian superconductor¹. It hosts Majorana zero modes at vortex cores, as in a $p_x + ip_y$ superconductor², but respects time-reversal symmetry. As argued in Ref. 1, the presence of superconductor induces a pairing interaction between the helical Dirac fermions at the surface of the topological insulator, and gaps out the surface spectrum. Then, the interface can be modeled elegantly by a simple matrix Hamiltonian in Nambu space (we follow the convention of Ref. 3),

$$H_{FK}(\mathbf{k}) = \begin{pmatrix} h_s(\mathbf{k}) & i\sigma_y \Delta_s \\ -i\sigma_y \Delta_s^* & -h_s^*(-\mathbf{k}) \end{pmatrix}, \quad (1)$$

where $\mathbf{k} = (k_x, k_y)$ is the two-dimensional momentum in the interface plane, σ_i are the Pauli matrices, $h_s(\mathbf{k})$ is the surface Hamiltonian for the topological insulator describing the helical Dirac fermions^{3,4},

$$h_s(\mathbf{k}) = -\mu_s + v_s(\sigma_x k_y - \sigma_y k_x). \quad (2)$$

Fu and Kane also proposed to use S-TI proximity structures to generate and manipulate Majorana fermions which obey non-Abelian statistics and are potentially useful for fault tolerant quantum computation¹. This proposal and a few others that followed based on superconductor-semiconductor heterostructures⁵⁻⁹ have revived the interest in superconducting proximity effect involving insulating/semiconducting materials with spin-orbit coupling. More complex S-TI proximity structures with ferromagnets^{10,11} or unconventional superconductors¹² have been investigated.

Given the importance of this proposal, it is desirable to understand to what extent the effective model H_{FK} holds, and what are the values of (Δ_s, μ_s, v_s) for given materials. Answering these questions is crucial for future experiments designed to probe and manipulate Majorana

fermions. As a first step in this direction, Stanescu et al considered a microscopic lattice model for the TI-S interface¹³. In this model, TI and S are described by a tight binding Hamiltonian defined on the diamond and hexagonal lattice respectively. The two materials are coupled by tunneling term in the Hamiltonian. These authors found that for small \mathbf{k} , $H_{FK}(\mathbf{k})$ is valid but its parameters are significantly renormalized by the presence of the superconductor. This is supported by leading order perturbation theory in the weak coupling (tunneling) limit. They also discussed the induced p -wave correlation within the framework of perturbation theory. The p -wave correlation has also been noted in an analogous proximity structure in two dimension between a quantum spin Hall insulator and a superconductor¹⁴.

In this work, we consider S-TI proximity structures where S and TI are *strongly* coupled to each other, rather than being separated by a tunneling barrier. This is the desired, presumably the optimal, configuration to realize the Fu-Kane proposal, e.g. to achieve maximum value of Δ_s in H_{FK} for given superconductor. In the strong coupling limit, the modification of superconductivity by the TI becomes important. This includes the suppression of the superconducting order parameter, the induction of triplet pair correlations by spin-active scattering at the interface, and the formation of interface states below the bulk superconducting gap. In order to accurately answer questions raised in the preceding paragraph for strongly coupled S-TI structures, one has to self-consistently determine the the spatial profile of the order parameter near the interface.

Our work is also motivated by recent experimental discovery that Copper-doped topological insulator $\text{Cu}_x\text{Bi}_2\text{Se}_3$ becomes superconducting at a few Kelvins^{15,16}. It seems possible then to combine such superconductors with topological insulator Bi_2Se_3 to achieve strong proximity coupling. Using Bi_2Se_3 and $\text{Cu}_x\text{Bi}_2\text{Se}_3$ as one of the examples, we set up microscopic, continuum models for the S-TI structures and solve the result Bogoliubov-de Gennes (BdG) equation

numerically. We first compute the superconducting order parameter as a function of the distance away from the interface. We then verify the validity of the Fu-Kane effective model and extract its parameters from the low energy sector of the energy spectrum. The emergence of H_{FK} will be viewed as the result of the “inverse proximity effect”, namely strong modification of superconductivity by the presence of TI. This is in contrast to the previous viewpoint of pairing between surface Dirac fermions, which is a more proper description in the tunneling limit. The spectral weight of these low energy modes (with energy below the bulk superconducting gap) are shown explicitly to peak near the interface but penetrate well into the superconductor. We will also show analytically that the induced triplet pair correlations are of $p_x \pm ip_y$ orbital symmetry, and systematically study their spatial and momentum dependence. Our results connect the phenomenological theory of Fu and Kane¹ to real materials. Our results for continuum models and strong coupling limit are also complementary to the results of Stanescu et al¹³ for lattice models and tunneling limit.

In what follows, we first outline the formulation of the problem and then present the main results. Technical details on numerically solving the BdG equation are relegated to the appendix.

II. MODEL AND BASIC EQUATIONS

The band gaps of topological insulators are much larger than the superconducting gap of all weak coupling s -wave superconductors. For the purpose of studying the proximity effect between such superconductors and topological insulators, it is sufficient to describe the topological insulator using the low energy effective $\mathbf{k} \cdot \mathbf{p}$ Hamiltonian. Following Zhang et al¹⁷, we model Bi_2Se_3 by

$$H_{TI}(\mathbf{k}) = \begin{pmatrix} M(\mathbf{k}) & 0 & A_1 k_z & A_2 k_- \\ 0 & M(\mathbf{k}) & A_2 k_+ & -A_1 k_z \\ A_1 k_z & A_2 k_- & -M(\mathbf{k}) & 0 \\ A_2 k_+ & -A_1 k_z & 0 & -M(\mathbf{k}) \end{pmatrix} - \mu \hat{I}. \quad (3)$$

Here $k_{\pm} = k_x \pm ik_y$, $M(\mathbf{k}) = M - B_1 k_z^2 - B_2(k_x^2 + k_y^2)$, and \hat{I} is 4×4 unit matrix. The numerical values of the parameters are obtained from first principle calculations^{17,18}, $M = 0.28$ eV, $A_1 = 2.2$ eVÅ, $A_2 = 4.1$ eVÅ, $B_1 = 10$ eVÅ², $B_2 = 56.6$ eVÅ². We work in basis $\{|1 \uparrow\rangle, |1 \downarrow\rangle, |2 \uparrow\rangle, |2 \downarrow\rangle\}$, where 1 (2) labels the $P1_z^+$ ($P2_z^+$) orbital¹⁷. Note that we have neglected the unimportant diagonal term $\epsilon_0(\mathbf{k})$ in Ref. 17 which only slightly modifies the overall curvature of the band dispersion. We also keep the chemical potential μ as a tuning parameter.

We consider a simple model of superconductor derived from a metallic state obtained by turning off the spin-orbit coupling ($A_1 = A_2 = 0$) in H_{TI} and tuning the Fermi level well into the conduction band²². The metal

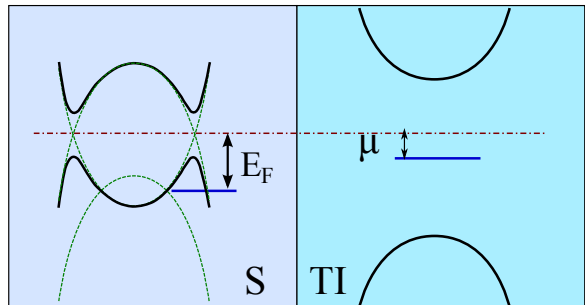


FIG. 1: Schematic (not to scale) band diagrams in a superconductor-topological insulator (S-TI) proximity structure. E_f is the Fermi energy of the metal described by H_M measured from the band crossing point. μ is the chemical potential of TI measured from the band gap center. The superconducting gap is much smaller than the band gap of TI.

Hamiltonian

$$H_M(\mathbf{k}) = \text{diag}[M(\mathbf{k}), M(\mathbf{k}), -M(\mathbf{k}), -M(\mathbf{k})] - E_f \hat{I}, \quad (4)$$

with $E_f > M$. This mimics electron-doping the topological insulator¹⁶ or equivalently electrochemically shifting its chemical potential by applying a gate voltage¹⁹. As shown in Fig. 1, the valence band (band 1 with dispersion $M(\mathbf{k}) - E_f$) is well below the Fermi level and remains inert as far as superconductivity is concerned. Next, within the framework of Bardeen-Cooper-Schrieffer theory, we assume attractive interaction between the electrons in the conduction band (band 2) near the Fermi surface described by the reduced Hamiltonian,

$$H_{int} = \sum_{\mathbf{k}} \psi_{2\uparrow}^\dagger(\mathbf{k}) \psi_{2\downarrow}^\dagger(-\mathbf{k}) \Delta + h.c. \quad (5)$$

Here Δ is the superconducting order parameter, $\psi_{l\sigma}^\dagger$ is the electron creation operator for orbital $l = 1, 2$ and spin $\sigma = \uparrow, \downarrow$. The superconductor is then described by

$$H_S = \sum_{\mathbf{k}, l, \sigma} \psi_{l\sigma}^\dagger(\mathbf{k}) H_M(\mathbf{k})_{l\sigma, l\sigma} \psi_{l\sigma}(\mathbf{k}) + H_{int}. \quad (6)$$

Note that H_S and H_{TI} are in the same basis.

This model is inspired partly by superconductor $\text{Cu}_x\text{Bi}_2\text{Se}_3$. The transition temperature at optimal doping $x = 0.12$ is $T_c = 3.8\text{K}$, which corresponds to a zero temperature superconducting gap $\Delta \sim 0.6\text{meV}$ ^{15,16}. The Fermi level is 0.25eV above the bottom of the conduction band, and the Fermi wave vector $k_f \sim 0.12\text{\AA}^{-1}$. The pairing symmetry of $\text{Cu}_x\text{Bi}_2\text{Se}_3$ is to our best knowledge not clear at present. If it turns out to be a conventional s -wave superconductor, its main features will be captured by H_S above with suitable choice of E_f and Δ .

Now consider a proximity structure consisting of a superconductor at $z < d$ and a topological insulator at $z > d$ (Fig. 1). The interface at $z = d$ is assumed to be specular, so the momentum $\mathbf{k}_{\parallel} = (k_x, k_y)$ parallel to the

interface is conserved. The Hamiltonian for the whole system

$$\begin{aligned} \mathcal{H} = & \int d\mathbf{k}_{\parallel} dz \left\{ \sum_{\sigma} \psi_{1\sigma}^{\dagger}(\mathbf{k}_{\parallel}, z) [h_0 - \mu(z)] \psi_{1\sigma}^{\dagger}(\mathbf{k}_{\parallel}, z) \right. \\ & - \sum_{\sigma} \psi_{2\sigma}^{\dagger}(\mathbf{k}_{\parallel}, z) [h_0 + \mu(z)] \psi_{2\sigma}^{\dagger}(\mathbf{k}_{\parallel}, z) \\ & + \Delta(z) \psi_{2\uparrow}^{\dagger}(\mathbf{k}_{\parallel}, z) \psi_{2\downarrow}^{\dagger}(-\mathbf{k}_{\parallel}, z) + h.c. \\ & + A_1(z) [\psi_{1\uparrow}^{\dagger}(-i\partial_z) \psi_{2\uparrow} + \psi_{1\downarrow}^{\dagger}(i\partial_z) \psi_{2\downarrow} + h.c.] \\ & \left. + A_2(z) [\psi_{1\uparrow}^{\dagger} k_{-} \psi_{2\downarrow} + \psi_{1\downarrow}^{\dagger} k_{+} \psi_{2\uparrow} + h.c.] \right\}. \quad (7) \end{aligned}$$

Here $h_0(\mathbf{k}_{\parallel}, \partial_z) = M - B_1 \partial_z^2 - B_2 k_{\parallel}^2$, $\mu(z)$ and $A_i(z)$ are piece-wise constant,

$$\mu(z) = E_f \theta(d - z) + \mu \theta(z - d), \quad (8)$$

$$A_i(z) = A_i \theta(z - d), \quad i = 1, 2 \quad (9)$$

in terms of the step function θ . The order parameter obeys the gap equation

$$\Delta(z) = g(z) \int d\mathbf{k}_{\parallel} \langle \psi_{2\uparrow}(\mathbf{k}_{\parallel}, z) \psi_{2\downarrow}(-\mathbf{k}_{\parallel}, z) \rangle. \quad (10)$$

We assume $g(z) = g\theta(d - z)$, the coupling constant g determines the bulk gap.

To self-consistently solve Eq. (7) and (10), we introduce Bogoliubov transformation

$$\psi_{l\sigma}(\mathbf{k}_{\parallel}, z) = \sum_n u_{n,l\sigma}(\mathbf{k}_{\parallel}, z) \gamma_{n,\mathbf{k}_{\parallel}} + v_{n,l\sigma}^*(\mathbf{k}_{\parallel}, z) \gamma_{n,\mathbf{k}_{\parallel}}^{\dagger} \quad (11)$$

to diagonalize \mathcal{H} as

$$\mathcal{H} = E_g + \int d\mathbf{k}_{\parallel} \sum_n \epsilon_n(k_{\parallel}) \gamma_{n,\mathbf{k}_{\parallel}}^{\dagger} \gamma_{n,\mathbf{k}_{\parallel}}, \quad (12)$$

where E_g is the ground state energy, and $\gamma_{n,\mathbf{k}_{\parallel}}^{\dagger}$ is the creation operator of Bogoliubov quasiparticles with energy $\epsilon_n(k_{\parallel})$. The wave function u and v satisfy the following Bogoliubov-de Gennes (BdG) equation,

$$\hat{H}_B(\mathbf{k}_{\parallel}, z) \hat{\phi}_n(\mathbf{k}_{\parallel}, z) = \epsilon_n(k_{\parallel}) \hat{\phi}_n(\mathbf{k}_{\parallel}, z). \quad (13)$$

Here, the BdG Hamiltonian

$$\hat{H}_B = \begin{pmatrix} h_0 - \mu & \mathbf{d} \cdot \boldsymbol{\sigma} & 0 & 0 \\ \mathbf{d} \cdot \boldsymbol{\sigma} & -h_0 - \mu & 0 & -\Delta i \sigma_y \\ 0 & 0 & \mu - h_0 & \mathbf{d} \cdot \boldsymbol{\sigma}^* \\ 0 & \Delta^* i \sigma_y & \mathbf{d} \cdot \boldsymbol{\sigma}^* & \mu + h_0 \end{pmatrix}, \quad (14)$$

and the wave function (dropping the arguments)

$$\hat{\phi}_n = (u_{n,1\uparrow}, u_{n,1\downarrow}, u_{n,2\uparrow}, u_{n,2\downarrow}, v_{n,1\uparrow}, v_{n,1\downarrow}, v_{n,2\uparrow}, v_{n,2\downarrow})^T. \quad (15)$$

The vector $\mathbf{d}(\mathbf{k}_{\parallel}, z)$ is defined as

$$d_x = A_1(z) k_x, \quad d_y = A_1(z) k_y, \quad d_z = A_2(z) (-i\partial_z). \quad (16)$$

Other quantities such as $h_0(\mathbf{k}_{\parallel}, z)$, $\mu(z)$, and $\Delta(z)$ are defined above. In terms of the wave functions, the zero temperature gap equation becomes

$$\Delta(z) = g(z) \int d\mathbf{k}_{\parallel} \sum_n' u_{n,2\uparrow}(\mathbf{k}_{\parallel}, z) v_{n,2\downarrow}^*(-\mathbf{k}_{\parallel}, z), \quad (17)$$

where the summation denoted by prime is restricted to $0 < \epsilon_n < \omega_D$ with ω_D being the Debye frequency.

We will exploit a particular symmetry of the BdG Hamiltonian to simplify calculations. Define the polar angle φ_k for the in-plane wave vector \mathbf{k}_{\parallel} ,

$$k_x + ik_y = k_{\parallel} e^{i\varphi_k}. \quad (18)$$

Then the BdG Hamiltonian for arbitrary (k_x, k_y) is related to that for $(k_x = k_{\parallel}, k_y = 0)$ by unitary transformation

$$\hat{U}^{\dagger}(\mathbf{k}_{\parallel}) \hat{H}_B(k_x, k_y) \hat{U}(\mathbf{k}_{\parallel}) = \hat{H}_B(k_{\parallel}, 0). \quad (19)$$

Here U is a block diagonal matrix,

$$U(\mathbf{k}_{\parallel}) = \text{diag}[e^{-i\sigma_z \frac{\varphi_k}{2}}, e^{-i\sigma_z \frac{\varphi_k}{2}}, e^{i\sigma_z \frac{\varphi_k}{2}}, e^{i\sigma_z \frac{\varphi_k}{2}}]. \quad (20)$$

Thus, the eigen energy ϵ_n only depends on the magnitude of \mathbf{k}_{\parallel} . Once the wave function for $\varphi_k = 0$ is known, the wave function for $\varphi_k \in (0, 2\pi)$ can be obtained by simple unitary transformation.

We solve the matrix differential equation (13) by conserving it into an algebraic equation, following the treatment of superconductor-ferromagnet structure by Halterman and Valls²⁰. The whole S-TI proximity structure is assumed to have finite dimension L in the z direction. The superconductor occupies the region $0 < z < d$, while the topological insulator occupies $d < z < L$. Hard wall boundary conditions are enforced at the end points, $z = 0$ and $z = L$. The exact boundary conditions at the end points only affect the local physics there, provided that the boundaries are sufficiently far away from the S-TI interface. We expand the wave function and order parameter in Fourier series²⁰,

$$u_{n,l\sigma}(z) = \sum_m u_{nm}^{l\sigma} \phi_m(z), \quad (21)$$

$$v_{n,l\sigma}(z) = \sum_m v_{nm}^{l\sigma} \phi_m(z), \quad (22)$$

$$\Delta(z) = \sum_m \Delta_m \phi_m(z), \quad (23)$$

$$\phi_m(z) = \sqrt{2/L} \sin(k_m z). \quad (24)$$

The integer $m = 1, 2, \dots, N$ labels the quantized longitudinal (along z) momentum $k_m = m\pi/L$. The cutoff N is chosen as²¹

$$B_1 k_N^2 = M + E_f + \omega_D. \quad (25)$$

By expansion Eq. (21)-(23), the BdG equation becomes an $8N \times 8N$ matrix equation. With a reasonable guess

of the order parameter profile, the eigen energies and eigen wave functions are obtained by solving the matrix eigen value problem. Then a new order parameter profile is computed from the gap equation. The procedure is iterated until convergence is achieved. Relevant technical details can be found in the appendix.

To analyze the spectrum of the system, it is convenient to define the retarded Green's function

$$G_{l\sigma}^R(\mathbf{k}_{\parallel}, z, t) = -i\theta(t)\langle\{\psi_{l\sigma}(\mathbf{k}_{\parallel}, z, t), \psi_{l\sigma}^{\dagger}(\mathbf{k}_{\parallel}, z, 0)\}\rangle \quad (26)$$

where the time-dependent field operators are in Heisenberg picture. For given \mathbf{k}_{\parallel} and z , the spectral functions are defined as

$$N_{l\sigma}(\mathbf{k}_{\parallel}, z, \omega) = -\text{Im}G_{l\sigma}^R(\mathbf{k}_{\parallel}, z, \omega), \quad (27)$$

$$N(\mathbf{k}_{\parallel}, z, \omega) = \sum_{l\sigma} N_{l\sigma}(\mathbf{k}_{\parallel}, z, \omega). \quad (28)$$

In terms of the wave functions and eigen energies,

$$N_{l\sigma}(\mathbf{k}_{\parallel}, z, \omega > 0) = \sum_n |u_{n,l\sigma}(\mathbf{k}_{\parallel}, z)|^2 \delta(\omega - \epsilon_n). \quad (29)$$

We also introduce the equal-time pair correlation functions for the conduction electrons

$$F_{\alpha\beta}(\mathbf{k}_{\parallel}, z) = \langle\psi_{2\alpha}(\mathbf{k}_{\parallel}, z)\psi_{2\beta}(-\mathbf{k}_{\parallel}, z)\rangle. \quad (30)$$

For example, at zero temperature we have

$$F_{\uparrow\uparrow}(\mathbf{k}_{\parallel}, z) = \sum_n^{\uparrow} u_{n,2\uparrow}(\mathbf{k}_{\parallel}, z)v_{n,2\uparrow}^*(-\mathbf{k}_{\parallel}, z), \quad (31)$$

$$F_{\downarrow\downarrow}(\mathbf{k}_{\parallel}, z) = \sum_n^{\downarrow} u_{n,2\downarrow}(\mathbf{k}_{\parallel}, z)v_{n,2\downarrow}^*(-\mathbf{k}_{\parallel}, z). \quad (32)$$

Triplet components of F will be induced near the S-TI interface by spin-active scattering²².

III. THE ORDER PARAMETER

First we present the spatial profile of the superconducting order parameter $\Delta(z)$ after the convergence is achieved. In all following calculations, E_f is fixed at 0.4eV, which is modeled after optimally doped $\text{Cu}_x\text{Bi}_2\text{Se}_3$ ¹⁶. And the Debye frequency is set as $\omega_D = 0.1E_f$ ²⁰. Fig. 2 shows an example with $\mu = 0$, $L = 300\text{nm}$, $d = 0.95L$, and a bulk gap of 0.6meV as found in $\text{Cu}_x\text{Bi}_2\text{Se}_3$. Going from the superconductor into the topological insulator, Δ first gets suppressed as the interface is approached before it drops to zero inside TI. The suppression is roughly 20% at the interface. Note that the fine wiggles of Δ in the simulation results are due to the finite momentum cutoff of the longitudinal momentum k_m . As previously discussed by Stojkovic and Valls²¹, the number of oscillations is $\sim N/2$, and the oscillation amplitude vanishes in the bulk as N is increased.

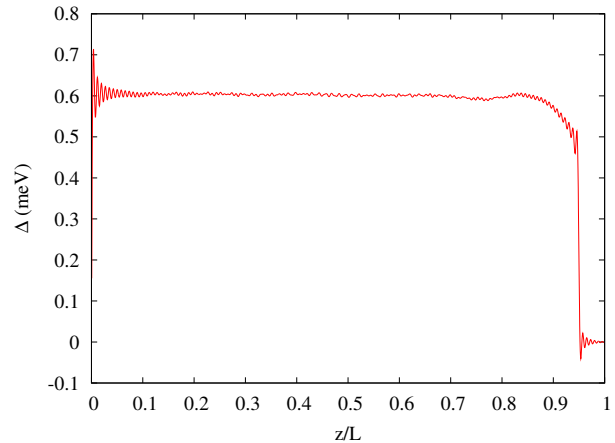


FIG. 2: The superconducting order parameter $\Delta(z)$ near an S-TI interface at $z = d = 0.95L$. The superconductor occupies $0 < z < d$, and topological insulator occupies $d < z < L$. $L = 300 \text{ nm}$, $\mu=0$, the bulk gap $\Delta_0 = 0.6\text{meV}$.

In this case, N is chosen to be 258 according to Eq. (25). So the matrix to be diagonalized is 2064 by 2064.

Fig. 3 show the result for $\mu = 0$, $d = 0.9L$, and a superconductor with bulk gap $\Delta_0 \sim 2.4\text{meV}$. Since the coherence length is much smaller than the previous example, it is sufficient to consider $L = 160\text{nm}$, and correspondingly $N = 138$. The order parameter profile depends weakly on μ , as shown in Fig. 4 for a superconductor with bulk gap $\sim 5.2\text{meV}$. From these examples, one observes that the length scale over which Δ is significantly suppressed does *not* scale with ξ_0 , the zero temperature coherence length of the superconductor. Rather it stays roughly the same, on the order of 30nm, as ξ_0 is varied over one decade from Fig. 2 to Fig. 4 (note the horizontal axis is z/L). This is not very surprising since ξ_0 is not the only length scale at play here. The interface represents a strong (as compared to Δ_0) perturbation that significantly distorts the bulk wave functions. The self-consistent microscopic BdG approach provides a reliable way to capture the details of $\Delta(z)$ near the interface.

It is illuminating to compare the proximity effect in S-TI structure with that in S-F structure²³, where F stands for a ferromagnetic insulator. The presence of F breaks time-reversal and spin rotation symmetry and significantly suppresses the order parameter. The suppression is sensitive to the spin mixing angle which is related to the band gap and exchange field of F²³. In contrast, despite the spin-active scattering of electrons by TI which introduces spin-flips and spin-dependent phase shifts²², spin-orbit coupling is not pair breaking. The suppression of Δ near the interface is to a large extent due to the reorganization of local wave functions enforced by the boundary conditions at $z = d$ for piece-wise potentials $\mu(z)$, $A_i(z)$, $g(z)$. It depends on for example how the wave functions decay inside the TI for given E_f and μ , and involves “high-energy” physics beyond the scale of Δ but below the scale of the band gap. To test this,

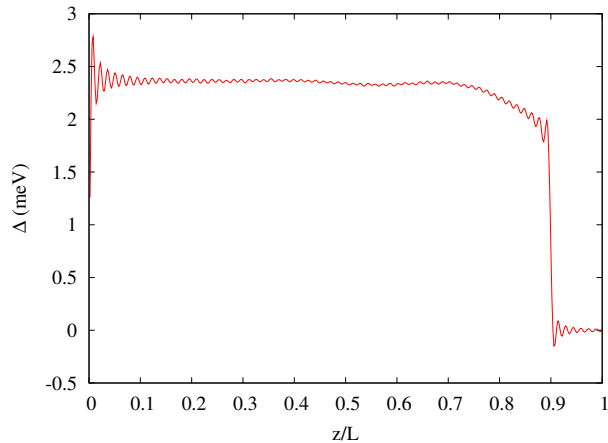


FIG. 3: The order parameter $\Delta(z)$ near an S-TI interface at $z = d = 0.9L$. $L = 160$ nm, $\mu=0$, $\Delta_0 \sim 2.4$ meV.

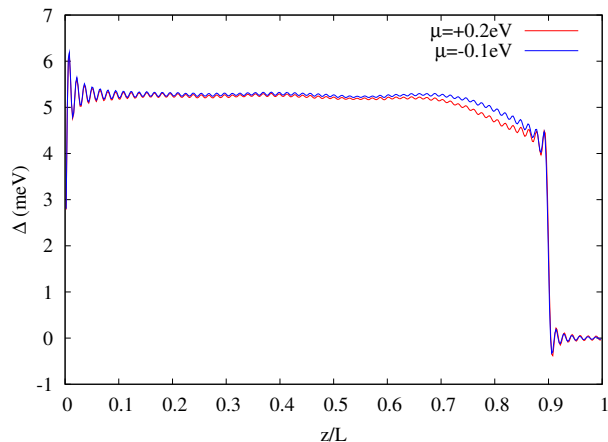


FIG. 4: The order parameter profile for two different chemical potentials of the topological insulator, $\mu = -0.1$ eV and $\mu = 0.2$ eV. $L = 160$ nm, $\Delta_0 \sim 5.2$ meV.

we have investigated the proximity effect between the same superconductor and a hypothetical ordinary insulator modeled by H_{TI} with $A_1 = A_2 = 0$ and the same band gap. The suppression of Δ by such an ordinary insulator turns out to be very similar.

IV. THE INTERFACE MODE AND THE FU-KANE MODEL

Next we analyze the energy spectrum of the system, $\epsilon_n(k_{\parallel})$, obtained from the BdG calculation. Take the case of $\mu = 0$, $L = 160$ nm, $d = 0.9L$, $\Delta_0 \sim 5.2$ meV as an example. Fig. 5 shows the first several energy levels of the composite system versus the transverse momentum k_{\parallel} . There are many continuously dispersing modes at energies above the bulk gap. They are the usual Bogoliubov quasiparticles for different quantized longitudinal

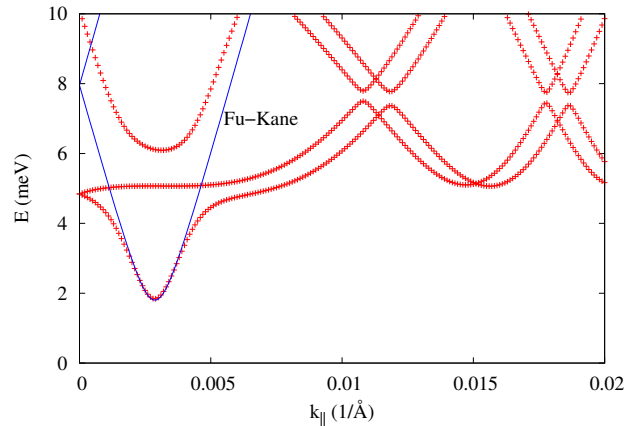


FIG. 5: The lowest few energy levels $\epsilon_n(k_{\parallel})$. $\mu = 0$, $L = 160$ nm, and the bulk superconducting gap $\Delta_0 \sim 5.2$ meV. A well-defined interface mode is clearly visible at sub-gap energies. Solid lines show a fit to the Fu-Kane model, with $\Delta_s = 1.8$ meV, $v_s = 2.7$ eVÅ, and $\mu_s = 7.5$ meV.

momenta. One also sees a series of avoided level crossings. At small k_{\parallel} emerges a well-defined mode below Δ_0 . We will identify it as the interface mode first discussed by Fu and Kane¹.

The Fu-Kane model Eq. (1) predicts the dispersion

$$E(k) = \sqrt{|\Delta_s|^2 + (v_s k \pm \mu_s)^2}. \quad (33)$$

We fit the very low energy portion of the spectrum to this prediction to extract the phenomenological parameters in the Fu-Kane model. The result is shown in Fig. 5. We find that, not surprisingly, $\Delta_s = 1.8$ meV which is much smaller than $\Delta_0 = 5.2$ meV, and $v_s = 2.7$ eVÅ which deviates significantly from $A_2 = 4.2$ eVÅ predicted for the surface dispersion of TI. Moreover, $\mu_s = 7.5$ meV despite that the chemical potential of TI is $\mu = 0$. Therefore, our results show that the values of (Δ_s, v_s, μ_s) are strongly renormalized by the presence of the superconductor. This is consistent with the findings of Stanescu et al for weakly coupled S-TI structures¹³.

We have checked the validity of the Fu-Kane model for a variety of chemical potentials. Representative examples are plotted in Fig. 6. In each case, the sub-gap mode can be well accounted by the Fu-Kane model with suitable choice of parameters. While μ_s is always different from μ , numerically we find it scales linearly with μ . At the same time, Δ_s and v_s show no strong dependence on μ for this set of parameters. To make sure that the sub-gap mode is indeed localized near the interface, we plot in Fig. 7 the z dependence of the spectral function $N(k_{\parallel}, z, \omega)$. The spectral weight of the sub-gap mode is peaked near the interface and decays over a length scale $\sim \xi_0$ into the superconductor. Note that the spectral weight on the TI side (not shown in the figure) is finite, but it is much smaller in magnitude and decays very fast inside TI.

We have carried out similar analysis for superconductors with larger coherence length. Fig. 8 shows the evo-

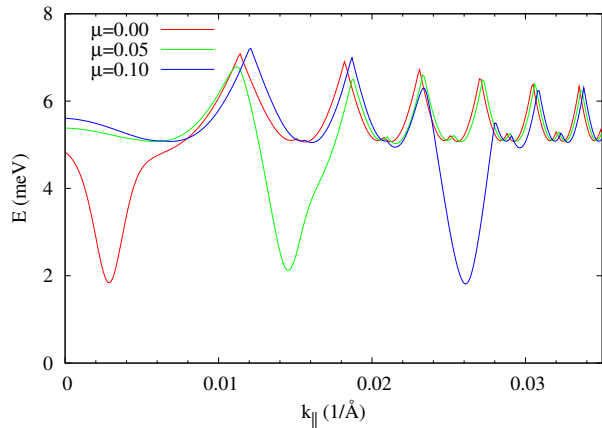


FIG. 6: The dispersion of the lowest energy level for different μ (in eV). Other parameters are the same as in Fig. 5, $L = 160\text{nm}$ and $\Delta_0 \sim 5.2\text{meV}$. Fu-Kane model well describes the lowest energy mode. As μ is increased, Δ_s and v_s stay roughly the same, while μ_s scales linearly with μ .

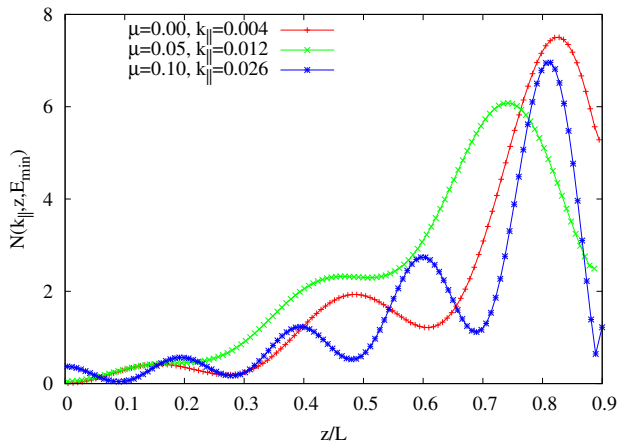


FIG. 7: The spectral function $N(k_{\parallel}, z, \omega)$ of the lowest energy level, $\omega = E_{\min}$, shown in Fig. 6. The interface is at $z = 0.9L$, $L = 160\text{nm}$. The spectral function oscillates rapidly with z , so only its envelope is plotted.

lution of the sub-gap mode with μ for $\Delta_0 = 2.4\text{meV}$. In this case, the values of (Δ_s, v_s, μ_s) all varies with μ . Superconductors with larger ξ_0 and smaller Δ_0 are thus more sensitive to changes in μ and other microscopic details near the interface. The exact values of the effective parameters in the Fu-Kane model in general depend on such microscopic details.

V. TRIPLET PAIR CORRELATIONS

It is well known that in heterostructures of s -wave superconductors, pairing correlations in other orbital channels, e.g. p -wave correlations, will be induced by scattering at the interfaces^{24,25}. For example, inver-

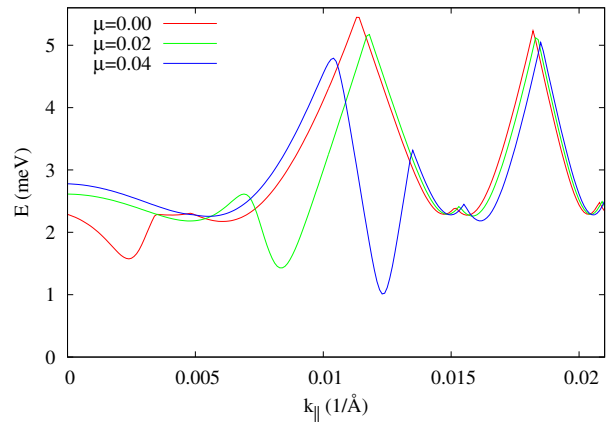


FIG. 8: The lowest energy level of an S-TI structure with $L = 160\text{nm}$, $d = 0.9L$, $\Delta_0 = 2.4\text{meV}$. μ is the chemical potential of the TI and measured in eV.

sion/reflection symmetry ($z \leftrightarrow -z$) is lost in an S-TI proximity structure, and the appearance of p -wave correlations seems natural from partial wave analysis. Moreover, scattering by a topological insulator is spin-active. The spin-orbit coupling inside a TI acts like a momentum-dependent magnetic field to flip the electron spin and introduce different phase shifts for spin up and down electrons. The scattering matrix has been worked out by us previously²². Thus, a singlet s -wave Cooper pair can be converted into a pair of electrons in spin-triplet state at the S-TI interface. However, it is important to recall that by assumption attractive interaction only exists (or is appreciable) in the s -wave channel. There is no binding force to sustain a triplet Cooper pair or a triplet superconducting order parameter. Similar (but different) pairing correlations in superconductor-ferromagnet hybrid structures have been extensively studied²⁴. The appearance of p -wave correlations in S-TI systems has been pointed out previously by Stanescu et al using a perturbative analysis¹³.

We focus on the equal-time pair correlation functions defined in Eq. (30). By exploiting the symmetry of the BdG Hamiltonian, Eq. (19), we are able to find analytically the orbital structure of the triplet correlation functions. The unitary transformation Eq. (20) yields

$$\begin{aligned} u_{2\uparrow}(k_x, k_y) &= u_{2\uparrow}(k_{\parallel}, 0)e^{-i\varphi_k/2}, \\ u_{2\downarrow}(k_x, k_y) &= u_{2\downarrow}(k_{\parallel}, 0)e^{+i\varphi_k/2}, \\ v_{2\uparrow}(k_x, k_y) &= v_{2\uparrow}(k_{\parallel}, 0)e^{+i\varphi_k/2}, \\ v_{2\downarrow}(k_x, k_y) &= v_{2\downarrow}(k_{\parallel}, 0)e^{-i\varphi_k/2}. \end{aligned} \quad (34)$$

Using these relations, we find

$$F_{\uparrow\uparrow}(\mathbf{k}_{\parallel}, z) = F_{\uparrow\uparrow}(k_{\parallel}, z)e^{-i\varphi_k}, \quad (35)$$

$$F_{\downarrow\downarrow}(\mathbf{k}_{\parallel}, z) = F_{\downarrow\downarrow}(k_{\parallel}, z)e^{+i\varphi_k}. \quad (36)$$

Namely $F_{\uparrow\uparrow}$ ($F_{\downarrow\downarrow}$) has $p_x - ip_y$ ($p_x + ip_y$) orbital symmetry.

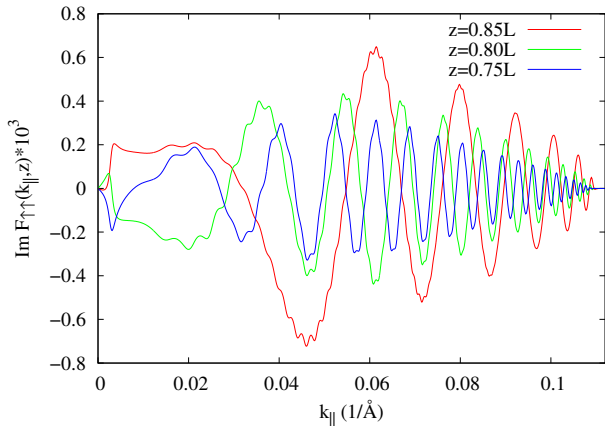


FIG. 9: The imaginary part of triplet pair correlation function $F_{\uparrow\uparrow}(k_{\parallel}, z)$. The S-TI interface is at $d = 0.9L$. $\mu = 0$, $L = 160\text{nm}$, $\Delta_0 = 5.2\text{meV}$.

Finally, the remaining triplet correlation function

$$\langle \psi_{2\uparrow}(\mathbf{k}_{\parallel}, z)\psi_{2\downarrow}(-\mathbf{k}_{\parallel}, z) + \psi_{2\downarrow}(\mathbf{k}_{\parallel}, z)\psi_{2\uparrow}(-\mathbf{k}_{\parallel}, z) \rangle \quad (37)$$

turns out to be zero. Note that the so-called odd-frequency pairing correlations^{24–26}, which vanishes in the equal-time limit, are also interesting in S-TI structures, but we will not discuss their behaviors here.

We find that $F_{\uparrow\uparrow}(k_{\parallel}, z)$ is purely imaginary and identical to $F_{\downarrow\downarrow}(k_{\parallel}, z)$. The results for $\mu = 0$, $L = 160\text{nm}$, $d = 0.9L$, $\Delta_0 = 5.2\text{meV}$ are plotted in Fig. 9. $F_{\uparrow\uparrow}$ vanishes at $k_{\parallel} = 0$ as well as for large k_{\parallel} , namely when $k_{\parallel} > \sqrt{(E_F + \omega_D + M)/B_2}$. This is consistent with lack of pairing in both limits. The behavior of $F_{\uparrow\uparrow}$ for small k_{\parallel} is illustrated in Fig. 10 for $\mu = 0$, $L = 300\text{nm}$, $d = 0.95L$, $\Delta_0 = 0.6\text{meV}$. As comparison, we also plotted the singlet pair correlation function

$$F_{\uparrow\downarrow}(\mathbf{k}_{\parallel}, z) = \sum_n^{\uparrow} u_{n,2\uparrow}(\mathbf{k}_{\parallel}, z)v_{n,2\downarrow}^*(-\mathbf{k}_{\parallel}, z) \quad (38)$$

which is s -wave and purely real.

VI. SUMMARY AND OUTLOOK

In summary, we have investigated the proximity effect between an s -wave superconductor and a topological insulator using a microscopic continuum model. Strong coupling between the two materials renders the surface state of TI a less useful concept for this problem. Our focus has been on the various modifications to superconductivity by the presence of TI. These include the suppression of the order parameter, the formation of interface modes below the bulk superconducting gap, and the induction of triplet pairing correlations. It is gratifying to see the Fu-Kane effective model emerges in the

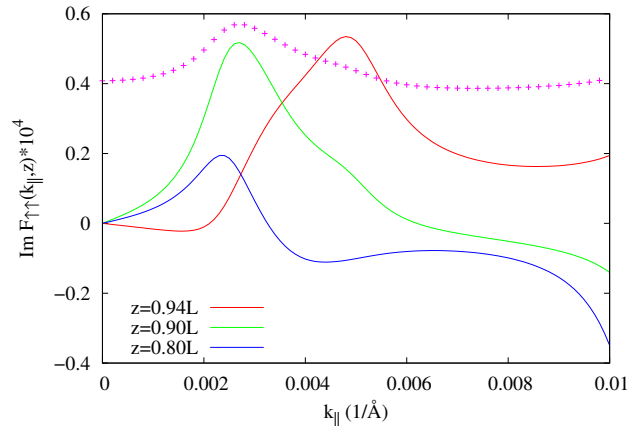


FIG. 10: The imaginary part of $F_{\uparrow\uparrow}(k_{\parallel}, z)$. $\mu = 0$, $L = 300\text{nm}$, $d = 0.95L$, $\Delta_0 = 0.6\text{meV}$. As comparison, the data points show the singlet pair correlation function $F_{\uparrow\downarrow}(k_{\parallel}, z = 0.9L)/3$.

low energy sector albeit with a set of renormalized parameters. Our results are complementary to previous theoretical work on the proximity effect^{1,13} and confirm the validity of the Fu-Kane model.

We made a few simplifying assumptions in our calculation. The superconductor is described by a two-band model with the valence band well below the Fermi level. Since only electrons near the Fermi surface are relevant for weak coupling superconductivity, we believe our main results are general. As idealizations, the chemical potential, the spin-orbit coupling, and the attractive interaction are assumed to be step functions with a sudden jump at the interface. More elaborate and realistic models can be considered within the framework of BdG equations. For example, one can add a tunneling barrier between S and TI, or include a Rashba-type spin-orbit coupling term (due to the gradient of chemical potential) at the interface. We will not pursue these generalizations here. Finally, the approach outlined here can be straightforwardly applied to study non-Abelian superconductivity in other superconductor-semiconductor heterostructures where spin-orbit coupling also plays a significant role^{5–9}.

VII. ACKNOWLEDGEMENTS

This work is supported by NIST Grant No. 70NANB7H6138 Am 001 and ONR Grant No. N00014-09-1-1025A.

Appendix

We follow the numerical scheme of Halterman and Valls to solve the matrix BdG equation²⁰. The wave functions and the order parameter are expanded in the

orthonormal basis $\{\phi_m(z)\}$, with $m = 1, \dots, N$. For example, function $u_{n,1\uparrow}(z)$ is represented by N numbers,

$$(u_{n,1}^{1\uparrow}, u_{n,2}^{1\uparrow}, \dots, u_{n,m}^{1\uparrow}, \dots, u_{n,N}^{1\uparrow}).$$

Accordingly, each term in \hat{H}_B is represented by a $N \times N$ matrix with the matrix elements given by

$$\begin{aligned} h_0(\mathbf{k}_{\parallel}, \partial_z) &\rightarrow \delta_{mm'}(M - B_1 k_m^2 - B_2 k_{\parallel}^2) \\ U(z) &\rightarrow E_f E_{mm'} + \mu F_{mm'} \\ A_2(z) \partial_z &\rightarrow A_2 G_{mm'} \\ A_1(z) k_{\pm} &\rightarrow A_z k_{\pm} F_{mm'} \\ \Delta &\rightarrow D_{mm'} \equiv \sum_{m''} J_{m,m',m''} \Delta_{m''} \end{aligned}$$

where

$$\begin{aligned} E_{mm'} &= \int_0^d \phi_m(z) \phi_{m'}(z) dz \\ F_{mm'} &= \int_d^L \phi_m(z) \phi_{m'}(z) dz \\ G_{mm'} &= \int_d^L \phi_m(z) \partial_z \phi_{m'}(z) dz \\ J_{m,m',m''} &= \int_0^d \phi_m(z) \phi_{m'}(z) \phi_{m''}(z) dz \end{aligned}$$

These integrals can be evaluated analytically. Then the BdG equation becomes an $8N \times 8N$ matrix equation. The gap equation can be rewritten as

$$\Delta_m = g \int d\mathbf{k}_{\parallel} \sum_n \sum_{m',m''} J_{m,m',m''} u_{nm'}^{2\uparrow}(\mathbf{k}_{\parallel}) v_{nm''}^{2\downarrow}(-\mathbf{k}_{\parallel})^*$$

The integral over \mathbf{k}_{\parallel} is first simplified to an integral over k_{\parallel} by the symmetry Eq. (19) and then evaluated numerically with high momentum cutoff $\sqrt{(E_F + \omega_D + M)/B_2}$.

-
- ¹ L. Fu and C. L. Kane, Phys. Rev. Lett. 100, 096407 (2008)
² N. Read and D. Green, Phys. Rev. B 61, 1026710297 (2000)
³ X.-L. Qi and S.-C. Zhang, arXiv:1008.2026
⁴ M. Z. Hasan and C. L. Kane, Rev. Mod. Phys. 82, 3045 (2010)
⁵ R. M. Lutchyn, J. D. Sau, and S. Das Sarma, Phys. Rev. Lett. 105, 077001 (2010)
⁶ J. D. Sau et al, Phys. Rev. B 82, 214509 (2010)
⁷ J. Alicea, Phys. Rev. B 81, 125318 (2010)
⁸ L. Mao, and C. Zhang, Phys. Rev. B 82, 174506 (2010)
⁹ L. Mao, J. Shi, Q. Niu, and C. Zhang, arXiv:1010.0932 (2010)
¹⁰ Y. Tanaka, T. Yokoyama, and N. Nagaosa, Phys. Rev. Lett. 103, 107002 (2009)
¹¹ J. Linder, Y. Tanaka, T. Yokoyama, A. Sudbo, and N. Nagaosa, Phys. Rev. B 81, 184525 (2010)
¹² J. Linder, Y. Tanaka, T. Yokoyama, A. Sudbo, and N. Nagaosa, Phys. Rev. Lett. 104, 067001 (2010)
¹³ T. D. Stanescu, J. D. Sau, R. M. Lutchyn, and S. Das Sarma, Phys. Rev. B 81, 241310 (2010)
¹⁴ A. M. Black-Schaffer, arXiv:1010.4625 (2010)
¹⁵ Y. S. Hor et al, Phys. Rev. Lett. 104, 057001 (2010)
¹⁶ L. A. Wray et al, Nature Physics 6, 855 (2010)
¹⁷ H. Zhang et al, Nature Physics 5, 438 (2009)
¹⁸ W. Zhang, R. Yu, H.-J. Zhang, X. Dai, and Z. Fang, New J. Phys. 12, 065013 (2010)
¹⁹ J. G. Checkelsky, Y. S. Hor, R. J. Cava, and N. P. Ong, arXiv:1003.3883
²⁰ K. Halterman and O. T. Valls, Phys. Rev. B 65, 014509 (2001)
²¹ B. P. Stojkovic and O. T. Valls, Phys. Rev. B 47, 5922 (1993)
²² E. Zhao, C. Zhang, and M. Lababidi, Phys. Rev. B 82, 205331 (2010)
²³ T. Tokuyasu, J. A. Sauls, and D. Rainer, Phys. Rev. B 38, 8823 (1988)
²⁴ M. Eschrig, T. Löfwander, T. Champel, J. C. Cuevas, J. Kopu, and G. Schön, J. Low Temp. Phys. 147, 457 (2007)
²⁵ A. A. Golubov, Y. Tanaka, Y. Asano and Y. Tanuma, J. Phys.: Condens. Matter 21, 164208 (2009)
²⁶ F. S. Bergeret, A. F. Volkov, and K. B. Efetov, Rev. Mod. Phys. 1321 (2005)